FAILURE ASSESSMENT FOR PIPES WITH COPLANAR CRACKS UNDER INTERNAL PRESSURE AND AXIAL TENSION

TEIK TIAN SEAH[1*] AND XUDONG QIAN[2]

[1]*INTECSEA SINGAPORE, 238164, Singapore*
E-mail: Teiktian.Seah@intecsea.com
[2]*Department of Civil & Environmental Engineering, National University of Singapore, 117576, Singapore*
E-mail: qianxudong@nus.edu.sg

The existing failure assessment diagram relies on the leading term characterizing the near-tip stress solutions, and ignores the geometry or plasticity-induced constraint variations. This paper aims to integrate the crack interaction effect between two coplanar cracks, measured by a constraint-based crack interaction factor, into the option 3 failure assessment curve in the engineering standard. This study examines circumferential coplanar embedded crack interacting with a surface crack in a pipe. This paper proposes a modified *J* solution based on the crack interaction factor to quantify the plasticity driven increase in the near-tip stress field for coplanar cracks. The stress field estimated based on this modified *J* solution agrees closely with the numerically computed stress field near the coplanar crack tips at different load levels. This work subsequently integrates the modified *J* solution into the failure assessment diagram.

Keywords: coplanar cracks, constraints, failure assessment diagram, pipelines; crack interaction, biaxial loading.

1 Introduction

Fracture failure for the fatigue or otherwise induced cracks has emerged as a primary failure mechanics in welded connection and pipes (Parool et al. 2017; 2018). Engineering assessment of the fracture resistance and fracture failure for pipes has become a critical challenge (Liu et al. 2019; 2019a). Non-destructive testing (Zhou et al 2018) often reveals multiple closely spaced cracks near the circumferential welds of the in-service pipelines. The possible interaction between these multiple cracks creates additional challenges in the integrity assessments of the welded pipelines, since the existing failure assessment procedure (BS7910 2015), which addresses the competing failure between plastic collapse and unstable fracture, relies on solutions derived from a single, stand-alone crack.

Previous efforts (Zhang et al 2015) in quantifying the interaction between closely located cracks have tried to examine the changes in the crack driving force, measured by either the stress intensity factor (K_I) or the energy release rate (*J*-integral), due to the presence of a nearby crack. Such efforts lead to the equivalent crack rule in engineering standard (BS7910 2015), which prescribes unnaturally a larger equivalent crack size for an increasing crack spacing. In addition, a previous study (Seah and Qian 2018) demonstrates a significant over-constraining effect in the

Proceedings of the 17th International Symposium on Tubular Structures.
Editors: X.D. Qian and Y.S. Choo

Published by Research Publishing, Singapore.
ISBN: 978-981-11-0745-0; doi:10.3850/978-981-11-0745-0_088-cd

near-tip stress field, which are not characterized by the K_I or J solutions. This implies that the exiting failure assessment diagram becomes un-conservative in assessing the coplanar cracks.

This study, hence, aims to integrate the previously reported over-constraining effect in the failure assessment framework for pipes with coplanar cracks near the circumferential welds. The pipes considered in this study experiences both the internal pressure and axial tension.

2 Modified *J*-Integral for Coplanar Cracks

2.1 *Crack interaction factor*

Seah and Qian (2018) has proposed a crack interaction factor to quantify the over-constraining effect in closely spaced co-planar cracks in plates. As the adjacent crack tip approaches the current crack tip, the J values computed from the coplanar cracks under-estimates this stress elevation near the crack tip (Seah and Qian 2018). The proposed crack interaction factor, ψ, characterizes the over-constraining effect caused by an adjacent crack tip based on the J-Q framework (O'Dowd and Shih, 1991; 1992),

$$\psi = \frac{\int_{x_1}^{x_2} \frac{\sigma_{\theta\theta,mc,\theta=0}}{\sigma_0} d\left(\frac{\sigma_0 r}{J}\right)}{\int_{x_1}^{x_2} \frac{\sigma_{\theta\theta,ref,\theta=0}}{\sigma_0} d\left(\frac{\sigma_0 r}{J}\right)} \tag{1}$$

where $\sigma_{\theta\theta,mc}$ refers to the opening stress near a crack tip influenced by an adjacent crack and $\sigma_{\theta\theta,ref}$ denotes the opening stress for a single crack in the same geometric configuration. ψ is an equivalent, normalized Q stress from $x_1 = \sigma_0 r / J = 2$ to x_2 along $\theta = 0$, where x_2 takes the minimum value of $\sigma_0 r / J = 10$ and the normalized distance at the smallest opening stress between the two crack tips.

2.2 *Modified J-Integral*

The above interaction factor quantifies the increase in the near-tip opening stress, which drives the extension of the crack and hence imposes a direct effect on the failure assessment procedure. To reflect this increase in the crack opening stress, the failure assessment curve requires an equivalent J-value based on the interaction factor for co-planar cracks. Assuming that the equivalent J-integral for a co-planar crack, J_{mod}, follows,

$$J_{mod} = \beta J_{ref} \tag{2}$$

Substituting J_{mod} into the HRR solution (Hutchinson, 1968; Rice and Rosengren, 1968) leads to,

$$\sigma_{mc,ij} = \beta^{\frac{1}{n+1}} \sigma_{sc,ij} \tag{3}$$

where $\sigma_{mc,ij}$ refers to the near-tip stress field in a multiple crack configuration, while $\sigma_{sc,ij}$ denotes that near a single crack. Substituting Eq. (3) into Eq. (1), we have,

$$\psi = \beta^{\frac{1}{n+1}} \rightarrow J_{\text{mod}} = \psi^{n+1} J_{ref} \tag{4}$$

3 Pipes with Coplanar Cracks

This section details the numerical model used to compute the crack interaction of the two coplanar circumferential cracks (embedded crack interacting with a surface crack) in a pipe. As illustrated in Figure 1a, the pipe has an outer diameter of 508 mm, and a wall thickness of 25.4 mm. The half length of the pipe is 2000 mm.

Figure 1b illustrates the crack front mesh simulated in ABAQUS (2014). The finite element model utilizes 8-node iso-parametric elements (C3D8 in the ABAQUS element library). The crack tip has a 1 μm keyhole radius and 40 rings of elements around the crack-tip. The *J*-integral is computed from the domain formed by the 40th ring of elements, over which *J*-integral converges among adjacent rings. The smallest element size near the crack tip equals 0.4 μm.

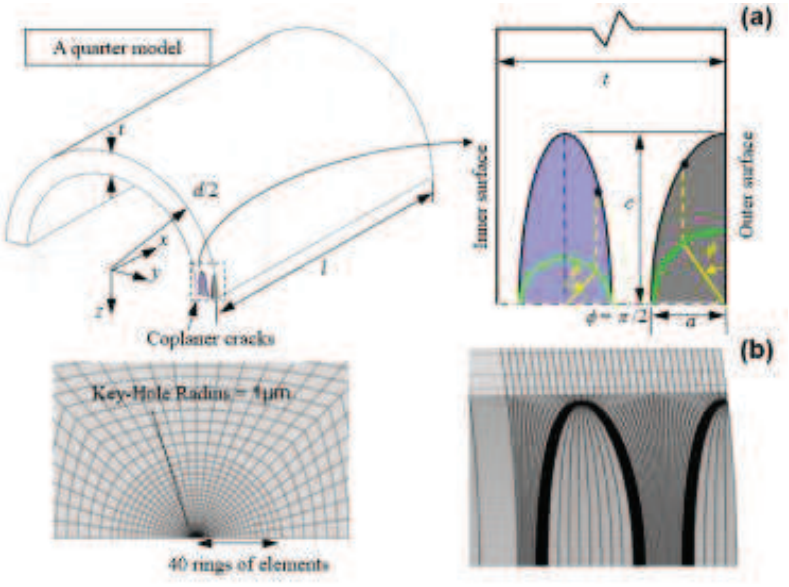

Figure 1. Coplanar crack in a pipe and the near-tip meshes.

The numerical analysis implements a non-proportional loading to simulate the combined action of the internal pressure and axial tension in two separate steps. The first loading step applies an internal pressure in the pipe with the end of the pipe restrained in the longitudinal direction. The second step applies a displacement-controlled axial tension to the end of the pipe.

The material true stress-true strain curve follows the Ramberg-Osgood relationship,

$$\frac{\varepsilon}{\varepsilon_0} = \begin{cases} \dfrac{\sigma}{\sigma_0} & \text{for } \sigma \le \sigma_0 \\ \dfrac{\sigma}{\sigma_0} + \alpha\left(\dfrac{\sigma}{\sigma_0}\right)^n & \text{for } \sigma > \sigma_0 \end{cases} \qquad \text{where } \alpha = 0.009 \tag{5}$$

where the yield strength of material, σ_0, equals 300 MPa with a Young's modulus of 207 GPa, and the strain-hardening exponent *n* equals 13 in this study.

Figure 2a and Figure 2b compare the near-tip stress for the embedded crack (at $\phi = \pi/2$) in Figure 1, the stress field estimated from the *J*-values for the coplanar cracks and that estimated using the J_{mod} value in Eq. (4). The estimation of the near-tip stress field utilizes the HRR

framework by substituting the different J values into the near-tip stress solution. The presence of a nearby surface crack elevates the near-tip stress of an embedded crack, compared to that of a single embedded crack. This elevation in the near-tip stress field increases with the increasing load, and stress field estimated from the domain integral value for the coplanar cracks (i.e., the J_{mc} value) under-estimates the opening stresses as shown in Figure 2b. The modified J value, J_{mod}, on the other hand, provides a reasonably accurate estimation of the near-tip opening stress at both nominal strain of 0.05% and 0.4%.

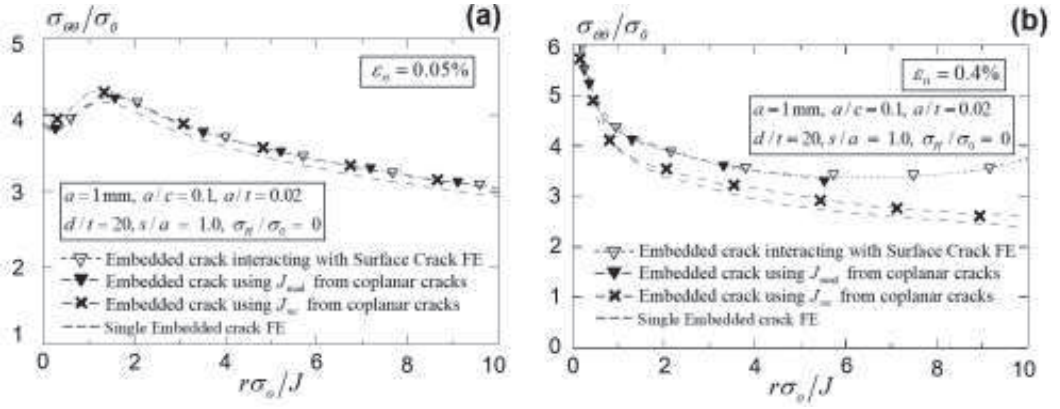

Figure 2. Near-tip stress field for an embedded crack interacting with a surface crack.

Figure 3 presents the ψ value calculated for the embedded crack (at $\phi = \pi/2$) in Figure 1 at increasing internal pressures σH/σ0. The ψ value increases with the nominal axial strain, εn, implying the plasticity dependent constraint variation for the coplanar cracks. The presence of the internal pressure creates a hoop stress, σH, in the pipe wall and hence a biaxial stress condition. Since the crack interaction factor ψ quantifies the plasticity-driven stress elevation near the tip of coplanar cracks, the presence of biaxial stresses impinges on the near tip stress field and increases the crack interaction factor, ψ.

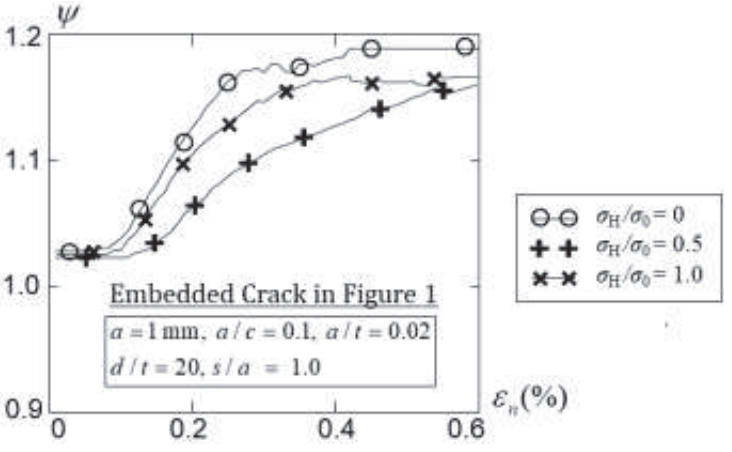

Figure 3. Crack interaction factor for an embedded crack interacting with a surface crack.

4 Implementation in Failure Assessment Diagram

4.1 *Definition of FAD*

This section details the procedure in applying the crack interaction factor, ψ, for engineering application via the failure assessment diagram. The failure assessment diagram (FAD) remains a common approach to assess the safety of a flaw, and has found wide applications for welded tubular joints (Qian et al. 2013; Qian 2013). This method considers two competing failure mechanisms: the brittle fracture and the plastic collapse. The *x*-axis of the FAD defines the non-dimensional load ratio,

$$L_r = \frac{\sigma_{ref}}{\sigma_0} \tag{6}$$

The *y*-axis quantifies the non-dimensional fracture ratio,

$$K_r = \frac{K_I}{K_{mat}} \tag{7}$$

where σ_{ref} refers to the reference stress at the flawed cross section, K_{mat} denotes the fracture toughness of the material, and K_I indicates the crack driving force. BS7910 (2015) has implemented three types of failure assessment curves (FACs), depending on the availability of the material and geometry information. The Option 1 and 2 FACs derive from the fitting solutions of the numerical database on a wide range of materials and plate type crack geometries. The Option 3 FAC is the material and geometry specific curve, derived from elastic plastic fracture mechanics,

$$f(L_r) = \begin{cases} \sqrt{J_e/J} & \text{for} \quad L_r < L_{r,\max} \\ 0 & \text{for} \quad L_r \geq L_{r,\max} \end{cases} \tag{8}$$

where J_e refers to linear-elastic *J*-integral and *J* denotes the total elastic-plastic *J*-value. The plastic collapse ratio, L_r, is limited to,

$$L_{r,\max} = \left(\sigma_y + \sigma_u\right) / 2\sigma_y \tag{9}$$

where σ_y and σ_u denote the material yield strength and ultimate strength, respectively.

4.2 *Modified FAC*

The modified *J* value, J_{mod}, described in Section 1, which considers the crack interaction factor, allows the redevelopment of the Option 3 failure assessment curves for coplanar cracks in a pipe to incorporate the over-constraining effect in coplanar cracks. Figure 2b confirms that the stress field estimated based on the J_{mod} value in Eq. (4) resembles closely the stress field near the tip of a coplanar crack. Substituting Eq. (4) into Eq. (8) leads to,

$$f(L_r)=\begin{cases}\dfrac{1}{\sqrt{\left(\psi/\psi_e\right)^{n+1}}}\sqrt{\dfrac{J_{e,sc}}{J_{sc}}} & \text{for} \quad L_r < L_{r,\max} \\ 0 & \text{for} \quad L_r \geq L_{r,\max}\end{cases} \tag{10}$$

where $J_{e,sc}$ refers to the J-integral calculated in the linear-elastic analysis for a single crack model, and ψ_e denotes the linear-elastic crack interaction factor. In Eq. (10), the approximate J-solution ($J_{mod}=\psi J_{sc}$) based on Eq. (4) has replaced the elastic-plastic crack driving force for the coplanar crack model.

Figure 4 presents the FAC for the embedded crack interacting with a surface crack (as illustrates in Figure 1) under combined internal pressure and axial tension. The FAC derives from the J and ψ solutions at the deepest crack-front location ($\psi = \pi/2$) in the embedded crack.

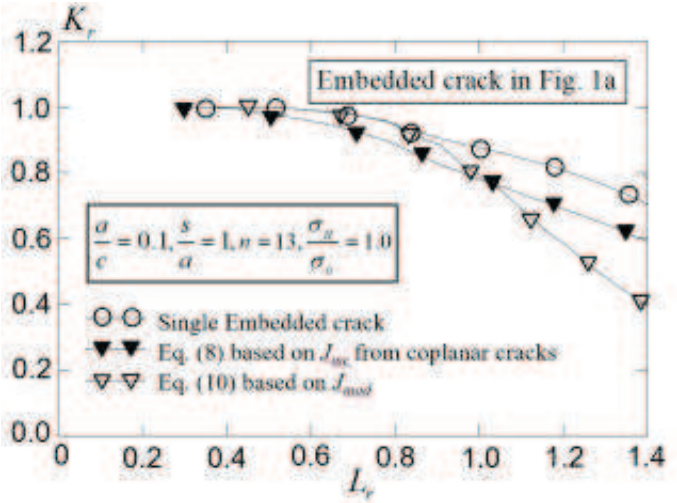

Figure 4. FAC for an embedded crack interacting with a surface crack

Due to the increasing constraint caused by the nearby surface crack, the modified FAC of the embedded crack based on J_{mod} value in Eq. (10), remains much lower than the FAC based on the J_{mod} solutions for the embedded coplanar cracks, using Eq. (8), at a large load ratio. At a small load ratio, the linear-elastic J_{mc} value does not quantify the increase in geometry constraint. On the other hand, the J_{mod} value incorporates this effect through the linear-elastic ψ_e value. Consequently, the FAC based on J_{mod} value in Eq. (10) locates above the FAC based on J_{mc} solutions, using Eq. (16), at a small load ratio.

5 Summary and Conclusions

This paper examines the interaction between coplanar circumferential embedded crack with surface crack in pipes under the combined internal pressure and axial tension. As the leading term in the near-tip stress field solution fails to quantify the crack-front constraint effect, the current study proposes an equivalent J value (J_{mod}) based on the crack interaction factor to facilitate its implementation in the failure assessment diagram. Based on this equivalent J-value, this study redevelops the option 3 FAC for circumferential coplanar cracks in pipes, and compares the newly developed FACs with the existing approach using J value (J_{mc}).

The failure assessment curve for embedded crack interacting with surface crack computed from the J_{mc} values is marginally than the proposed FAC based on the crack interaction factor, ψ, for small to intermediate load ratios, but becomes un-conservative at a large load ratio.

Acknowledgement

The authors would like to acknowledge the National University of Singapore for the support on the above study.

References

Ahmed, A and Qian, X. A deformation limit based on failure assessment diagram for fatigue cracked X-joints under in-plane bending. *Ships Offshore Struct*, 2015, 11, 182-197.

British Standard Institute. BS 7910. Guideline on Methods for Assessing the Acceptablility of Flaws in Metallic Structures. 2015.

Dassault Systèmes Simulia Corp. Abaqus Analysis User's Guide. Version 6.14. Providence, RI, USA. 2014.

Hutchinson JW. Singular behaviour at the end of a tensile crack in a hardening material. *J Mech Phys Solids*, 1968, 16, 13-31.

Liu, T. Y., Qian, X., Wang, W. and Chen, Y. Y. A node release approach to estimate J-R curve for single-edge-notched tension specimen under reversed loading. *Fatigue Fract Eng Mater Struct*, 2019, 42(7), 1595-1608.

Liu, T. Y., Qian, X., Wang, W. and Chen, Y. Y. Fracture resistance curve for single edge notched tension specimens under low cycle actions. *Eng Fract Mech*, 2019a, 211, 47-60.

O'Dowd NP, Shih CF. Family of crack-tip fields characterized by a triaxiality parameter-I. Structure of fields. *J Mech Phys Solids*, 1991, 39, 989-1015.

O'Dowd NP, Shih CF. Family of crack-tip fields characterized by a triaxiality parameter-II. Fracture Applications, *J Mech Phys Solids*, 1992, 40, 939-963.

Parool N, Qian X, Koh CG. An η-compliance method to estimate the J-Δa curve for pipes with a circumferential surface crack. *Fatigue Fract Eng Mater Struct*, 2017, 40, 1624-1639.

Parool N, Qian X, Koh CG. A modified hybrid method to estimate fracture resistance curve for pipes with a circumferential surface crack. *Eng Fract Mech*, 2018, 188, 1-19.

Qian, X., Li, Y. and Ou, Z. Ductile tearing assessment of high-strength steel X-joints under in-plane bending. *Eng Fail Anal*, 2013, 28, 176-191.

Qian, X. Failure assessment diagrams for circular hollow section X- and K-joints. *Int J Pres Ves Pip*, 2016, 104, 43-56

Rice JR, Rosengren GF. Plane strain deformation near a crack tip in a pwer-law hardenining material. *J Mech Phys Solids*, 1968, 16, 1-12.

Seah TT, Qian X. An interaction factor to estimate the over-constraining effect in plates with co-planar cracks. *Eng Fract Mech*, 2018, 199, 13-28.

Zhou, Y. L., Qian, X., Birnie, A. and Zhao, X. L. A reference free ultrasonic phased array to identify surface cracks in welded steel pipes based on transmissibility. Int J Pres Ves Pip, 2018, 168, 66-78.

Zhou, Y. L., Qian, X., Birnie, A. and Zhao, X. L. A reference free ultrasonic phased array to identify surface cracks in welded steel pipes based on transmissibility. *Int J Pres Ves Pip*, 2018, 168, 66-78.